

OPEN

Effect of confinement potential shape on the electronic, thermodynamic, magnetic and transport properties of a GaAs quantum dot at finite temperature

K. Luhlul Jahan¹, Bahadir Boyacioglu^{2*} & Ashok Chatterjee¹

The effect of the shape of the confinement potential on the electronic, thermodynamic, magnetic and transport properties of a GaAs quantum dot is studied using the power-exponential potential model with steepness parameter p . The average energy, heat capacity, magnetic susceptibility and persistent current are calculated using the canonical ensemble approach at low temperature. It is shown that for soft confinement, the average energy depends strongly on p while it is almost independent of p for hard confinement. The heat capacity is found to be independent of the shape and depth of the confinement potential at low temperatures and for the magnetic field considered. It is shown that the system undergoes a paramagnetic-diamagnetic transition at a critical value of the magnetic field. It is furthermore shown that for low values of the potential depth, the system is always diamagnetic irrespective of the shape of the potential if the magnetic field exceeds a certain value. For a range of the magnetic field, there exists a window of p values in which a re-entrant behavior into the diamagnetic phase can occur. Finally, it is shown that the persistent current in the present quantum dot is diamagnetic in nature and its magnitude increases with the depth of the dot potential but is independent of p for the parameters considered.

The subject of quantum dots (QDs) has attracted unprecedented attention for its fundamental appeal and technological potential¹. One of the most important advantages with quantum dots is that its shape and size can be controlled according to the desired properties. It is, of course, essential to know the nature of the confinement potential to formulate any theory of quantum dots. Early experiments indicated that the confinement potential in a quantum dot is essentially harmonic. Consequently, a large body of literature has piled up on the subject of parabolic quantum dots²⁻¹⁶. However, some recent experiments have suggested that the confinement potential in a quantum dot is rather anharmonic and has a finite depth^{17,18}. Adamowsky *et al.*¹⁷ suggested an attractive Gaussian potential model for confinement which has been found to be more realistic. Subsequently, extensive investigations¹⁹⁻³⁷ have been made on several properties of QDs using the Gaussian confinement potential. Ciurla *et al.*³⁸ have studied the problem of confinement potential profile in QDs and proposed a new class of confinement potentials, called the power-exponential (PE) potentials, which are sufficiently flexible to approximate the realistic confinement potentials in the QDs. They showed that the commonly used model confinement potentials, i.e. the parabolic and rectangular potential wells, could be obtained as the limiting forms of the power-exponential. Kwaśniowski and Adamowski³⁹ have studied the exchange interaction for electrons in coupled QDs by a configuration interaction method using confinement potentials with different profiles. The photoionization of a donor impurity in a power-exponential quantum dot (PEQD) has been studied by Xie⁴⁰ by using the PE potential model and the results have been presented as a function of the diffusion photon energy. It has been shown that the Photoionization Cross Section of a donor impurity in a QD is strongly dependent on the shape of the PE potentials, the geometrical size, and the impurity ion position.

¹School of Physics, University of Hyderabad, Hyderabad, 500 046, India. ²Vocational School of Health Services, Ankara University, 06290, Kecioren, Ankara, Turkey. *email: bboyacioglu@ankara.edu.tr

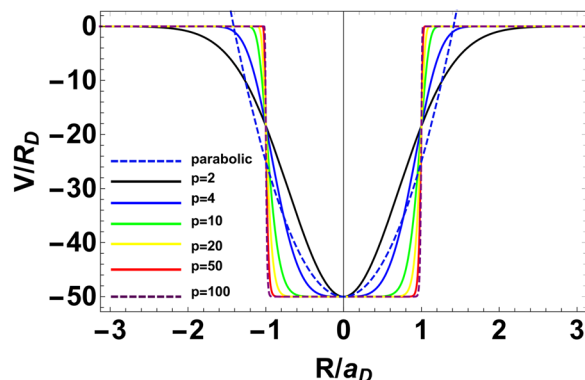


Figure 1. The shape of parabolic and the power-exponential confinement potential for $p = 2, 4, 10, 20, 50$ and 100 . The donor Bohr Radius a_D is the unit of length and the donor Rydberg R_D is the unit of energy³⁸.

To our knowledge, no investigation has so far been made on the temperature-dependent electronic, thermodynamic, magnetic and transport properties of a PEQD. In the present paper, we shall make an attempt in this direction in the presence of the spin-Zeeman interaction.

Model

The Hamiltonian of a system of an electron moving in a two-dimensional (2D) confining potential (ρ) in the presence of an external magnetic field, \mathbf{B} may be written as

$$H = \frac{1}{2m^*} \left(\mathbf{p} + \frac{e}{c} \mathbf{A} \right)^2 + V(\rho), \quad (1)$$

where ρ refers to the position vector of an electron in two dimensions, \mathbf{p} is the corresponding momentum operator, m^* is the electron effective mass and \mathbf{A} is the vector potential corresponding to the magnetic field \mathbf{B} which has been applied in the z direction. Choosing the gauge of \mathbf{A} as $\mathbf{A} = (-By/2, Bx/2, 0)$ such that \mathbf{A} is divergence-less and including the spin-Zeeman term, we can write Hamiltonian (1) as

$$H = -\frac{\hbar^2}{2m^*} \nabla_\rho^2 + V(\rho) + \frac{1}{8} m^* \omega_c^2 \rho^2 + \frac{1}{2} \hbar \omega_c (\hat{L}_z + g^* \hat{S}_z), \quad (2)$$

where L_z is the z -component of the angular momentum of the electron, ω_c is the bare cyclotron frequency given by $\omega_c = eB/m^*$ and $V(\rho)$ is the spherically symmetric PE potential³⁸ given by

$$V(\rho) = -V_0 e^{-\left(\frac{\rho}{R}\right)^p}, \quad (3)$$

where V_0 denotes the depth of the potential, R gives a measure of the range of the potential and thus represents the effective confinement length or the size of the QD and the parameter p decides the shape of the confinement potential and gives a measure of the steepness of the potential at the QD boundary. The smaller (larger) is the value p , the softer (harder) is the potential. For $p = 2$, the confinement potential has the Gaussian shape. This potential is soft, that is the potential has a fairly small steepness at the QD boundary. For $p \geq 4$ the confinement potential becomes hard that is the potential at the QD boundary becomes very steep. For $p \geq 10$, one deals with a very hard, rectangular-type confinement potential (Fig. 1).

Formulation

We assume that the deviation of the shape of the PE potentials from the parabolic potential is small enough so that it can be treated as a parabolic potential plus a perturbation. This is a reasonable assumption for small r and since in a QD, r would be generally small, it can be considered as a fairly good approximation. So we rewrite the Hamiltonian (1) as

$$H = H_0 + H_1, \quad (4)$$

with

$$H_0 = -\frac{\hbar^2}{2m^*} \nabla_\rho^2 + \frac{1}{2} m^* \omega_c^2 \rho^2 + \frac{1}{2} \hbar \omega_c (\hat{L}_z + g^* \hat{S}_z) - V_0, \quad (5)$$

$$H_1 = -\lambda \left[\frac{1}{2} m^* \omega_c^2 \rho^2 + V_0 \left(e^{-\left(\frac{\rho}{R}\right)^p} - 1 \right) \right], \quad (6)$$

where

$$\tilde{\omega}^2 = \omega_h^2 + \frac{\omega_c^2}{4}, \quad \omega_h^2 = \frac{V_0}{m^*R^2}, \quad (7)$$

and $\lambda = 0$ for a parabolic confinement and $\lambda = 1$ for the PE potential. We assume that the sole effect of H_1 is to renormalize the frequency $\tilde{\omega}$. So we treat H_1 at the mean field level. More specifically we write H_1 as

$$H_1 = \lambda \left[\frac{V_0}{\langle \rho^2 \rangle} - \frac{1}{2} m^* \omega_h^2 - V_0 \frac{\langle e^{-(\rho/R)^p} \rangle}{\langle \rho^2 \rangle} \right] \rho^2, \quad (8)$$

where $\langle \rho^2 \rangle$ is the expectation value of ρ^2 with respect to the wave function of the harmonic oscillator of frequency $\tilde{\omega}$. The problem now reduces to an effective parabolic problem described by the Hamiltonian

$$H = -\frac{\hbar^2}{2m^*} \nabla_\rho^2 + \frac{1}{2} m^* \omega^2 \rho^2 + \frac{1}{2} \hbar \omega_c (\hat{L}_z + g^* \hat{S}_z) - V_0, \quad (9)$$

where ω is the effective frequency and g^* is the effective Lande-g factor (which is equal to -0.44 for GaAs). The effective problem now satisfies the Schrödinger equation

$$H \Psi_{nls}(\rho, \theta, \sigma) = E_{nls} \Psi_{nls}(\rho, \theta, \sigma), \quad (10)$$

where $\Psi_{nls}(\rho, \theta, \sigma)$ is the wave function given by the Fock–Darwin states^{41,42}

$$\Psi_{nls}(\rho, \theta, \sigma) = \sqrt{\frac{\alpha^2 n!}{(n + |l|)! \pi}} (\alpha \rho)^{|l|} L_n^{|l|}(\alpha^2 \rho^2) e^{-\frac{\alpha^2}{2} \rho^2 + i l \theta} \chi_s(\sigma), \quad (11)$$

where $\alpha = (m^* \omega / \hbar)^{1/2}$, n is the radial quantum number, $l (= 0, \pm 1, \pm 2, \dots)$ is the azimuthal angular momentum quantum number, $L_n^{|l|}$ is the associated Laguerre polynomial, $\chi_s(\sigma)$ is the eigenstate of the spin operator with eigenvalue $s = \pm(1/2)$ and E_{nls} is given by^{41,42}

$$E_{nls} = (2n + |l| + 1) \hbar \omega + \frac{1}{2} \hbar \omega_c (l + g^* s) - V_0. \quad (12)$$

At zero temperature, the magnetization and the magnetic susceptibility of a system in a state (n, l) are defined by

$$M_{nl}(B) = -\frac{\partial E_{nl}}{\partial B}; \quad \chi = \frac{\partial M}{\partial B} \quad (13)$$

The partition function for the present system can be exactly calculated and is given by

$$Z(T, B) = \sum_{n=0}^{\infty} \sum_{l=0}^{\pm\infty} \sum_{s=-1/2}^{s=1/2} e^{-\beta E_{nls}} \quad (14)$$

where $\beta = 1/k_B T$. The partition function can be used to obtain the average energy, magnetization, magnetic susceptibility and heat capacity as

$$\langle E \rangle = -\frac{1}{Z} \left(\frac{\partial Z}{\partial \beta} \right); \quad \langle M \rangle = \frac{1}{\beta Z} \left(\frac{\partial Z}{\partial B} \right); \quad \chi = \frac{\partial \langle M \rangle}{\partial B}; \quad C = \frac{\partial \langle E \rangle}{\partial T}. \quad (15)$$

We are also interested in the temperature dependent persistent current and therefore we calculate the canonical ensemble average of J_{nl}^{spin} as follows:

$$\langle J_{nl}^{spin} \rangle = \frac{\sum_{n,l,s} J_{nl}^{spin} e^{-\beta E_{nls}}}{\sum_{n,l,s} e^{-\beta E_{nls}}}. \quad (16)$$

Numerical Results and Discussion

Before we present our results on magnetization and susceptibility, it may be worthwhile to show that the approximation made in Eq. (8) for H_1 is fairly good. To that end, we shall compare our present results (with $B = 0$) for the ground state energy with the ones obtained by the Ritz variational calculation performed by us and with those of Ciurla *et al.*³⁸ obtained using the high-order finite-difference method. Figure 2 shows the comparison for different values of p with $V_0 = 50R_D$ and $R = a_D$. It is clearly evident that our results are better than the variational results and are in good agreement with those of Ciurla *et al.*³⁸. This imparts a fair amount of confidence in our approximation for the ground state calculation. However, our approximation turns out to be not so good for the excited states.

In Fig. 3 we show the variation of magnetization for GaAs PEQD um dot as a function of the magnetic field for PE potentials for the ground state. The first observation we make here is that the magnitude of magnetization ($|M|$) in a QD increases with the increase in the magnetic field for a given value of V_0 and R for PE potentials.

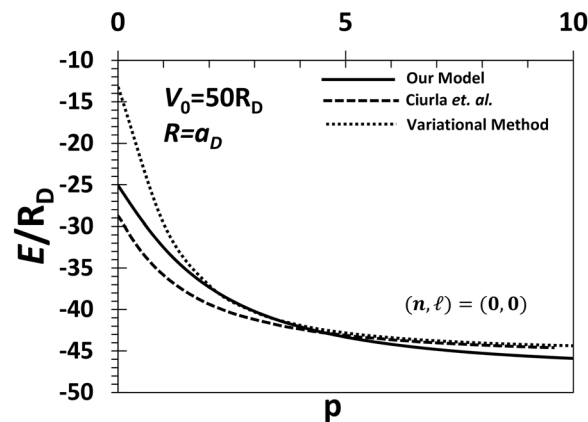


Figure 2. Ground state energy of a QD with the power-exponential potential as a confinement potential as a function of the shape of the potential (p) in the absence of the magnetic field with $V_0 = 50R_D$ and $R = a_D$.

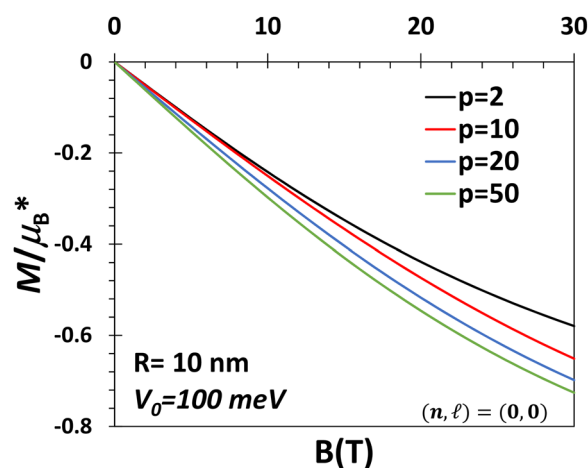


Figure 3. M vs. B for the GS of a QD with $V_0 = 100$ meV, $R = 10$ nm and $p = 2, 10, 20$ and 50 .

This is of course understandable. Also one can see the system is always in a diamagnetic state. This is again understandable in view of the inherent diamagnetism of the electron in a potential and the absence of paramagnetism in the GS. $|M|$ increases with the applied magnetic field which is again an expected behavior. The figure also shows that as the magnetic field increases, $|M|$ increases with p . Figure 4 shows the behavior of the susceptibility as a function of the magnetic field.

In Fig. 5 we plot the average thermal energy ($\langle E \rangle$) of an electron in a GaAs QD as a function of the parameter p for $B = 1$ T, $T = 1$ K, $R = 10$ nm and for three values of V_0 . One may observe that $\langle E \rangle$ increases monotonically as p decreases. Thus the average energy is higher if the potential is softer. The increase in $\langle E \rangle$ with decreasing p is sharp and substantial for small p and large V_0 . This is because as the potential becomes softer, it can accommodate a larger number of bound states at the Rydberg levels leading to a larger $\langle E \rangle$.

Figure 6 shows the variation of the average magnetization of a GaAs QD with $V_0 = 300$ meV as a function of B for several values of p at $T = 1$ K. $\langle M \rangle$ initially increases with B , reaches a maximum at a certain value of B and at low values of B , $\langle M \rangle$ is essentially independent of p . Above a certain value of B , $\langle M \rangle$ decreases with a further increase in B and becomes negative and continues to become more and more negative with increasing B . The behaviour is qualitatively different for different p values. Quantitatively, however, as p increases, $\langle M \rangle$ becomes negative at lower values of B and thus attains a larger negative value for the same value of B . In Fig. 7, we study the same $\langle M \rangle$ vs B graph for $V_0 = 50$ meV. It is interesting to see that for a shallow quantum dot, the shape does not play much significant role. This is also an expected behaviour. In Fig. 8, we show the variation of the average magnetization ($\langle M \rangle / \langle \mu \rangle_B$) directly as a function of the parameter p for a GaAs QD with $R = 10$ nm, $V_0 = 50, 100, 300$ meV and $B = 1$ T and $T = 1$ K. The magnetization remains positive all through in conformity with Fig. 7. Furthermore, at small p , $\langle M \rangle$ increases with p , attains a maximum and then decreases with the further increase in p and finally saturates to a constant value. When p becomes large, the confinement potential becomes very steep at the boundary mimicking a rectangular potential and in this case, only a few low-lying discrete states, contribute to the average energy because of the fast exponential decaying of the Boltzmann factor for the higher excited states. This explains the saturation of the magnetization with p . The maximum in $\langle M \rangle$ tends to flatten out as V_0 decreases. At small p ,

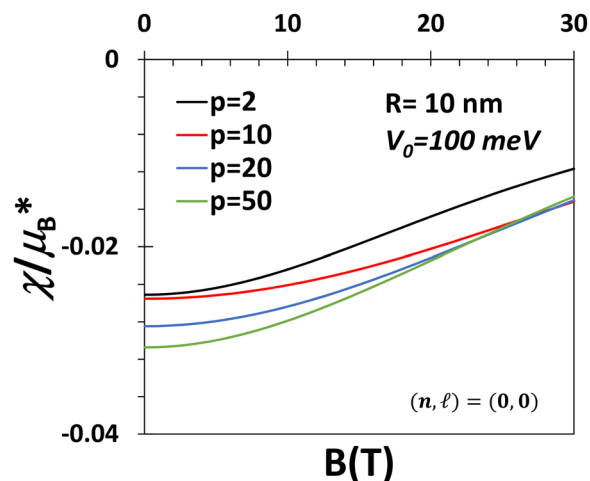


Figure 4. χ vs B for the GS of a QD with $V_0 = 100$ meV, $R = 10$ nm and 50 for $p = 2, 10, 20$ and 50.

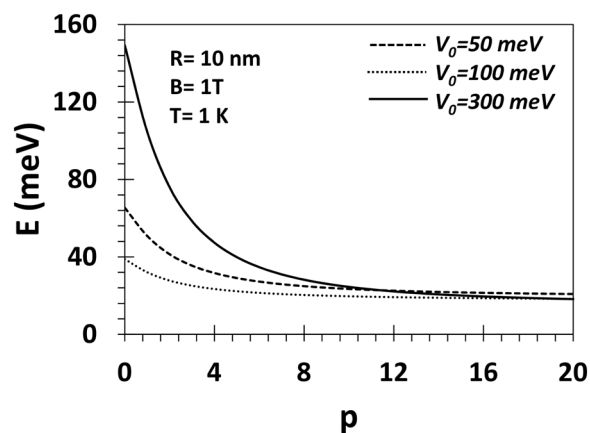


Figure 5. E vs p for a GaAs QD with $V_0 = 50, 100, 300$ meV, $R = 10$ nm, $B = 1$ T and, $T = 1$ K.

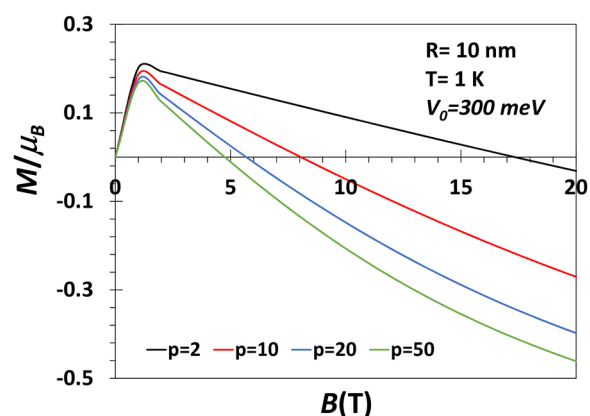


Figure 6. M vs B for a GaAs QD with $V_0 = 300$ meV, $R = 10$ nm, $B = 1$ T and $p = 2, 10, 20, 50$ at $T = 1$ K.

$\langle M \rangle$ increases with V_0 . This is because at small p , with increasing V_0 many more Rydberg-like states are supported by the potential. Thus as p exceeds a certain value, for large V_0 , we observe a crossing behaviour.

In Fig. 9 we plot the magnetic susceptibility (χ) of a GaAs QD as a function of B for $p = 2, 10, 20, 50$ at $T = 1$ K. The figure shows that at very low magnetic field the susceptibility is paramagnetic for QDs of all geometries. As B increases, χ decreases and at a certain critical value of B which depends weakly on the value of the shape parameter, χ becomes diamagnetic. As B increases further, χ saturates to a constant diamagnetic value. χ vs B

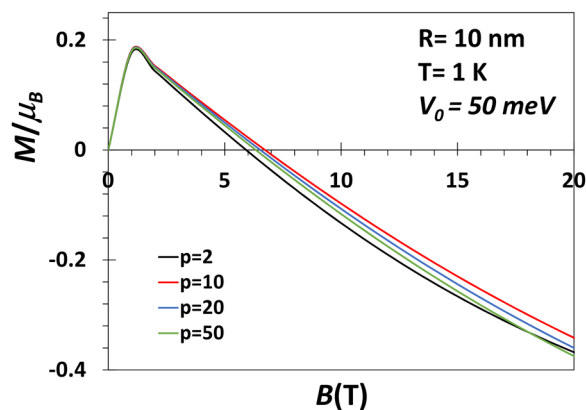


Figure 7. M vs B for a GaAs QD with $V_0 = 50$ meV, $R = 10$ nm, $B = 1$ T and $p = 2, 10, 20, 50$ at $T = 1$ K.

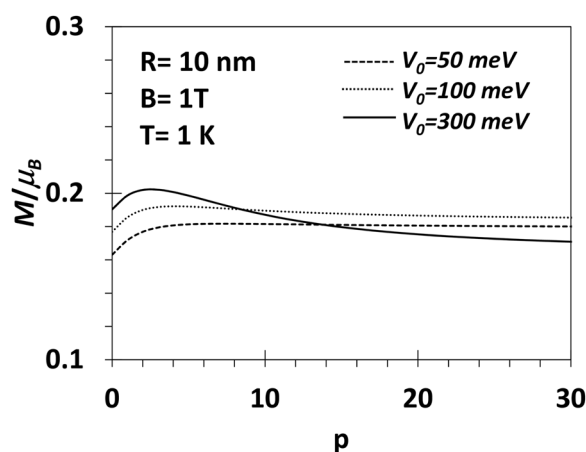


Figure 8. M vs p for a GaAs QD with $V_0 = 50, 100, 300$ meV, $R = 10$ nm, $B = 1$ T.

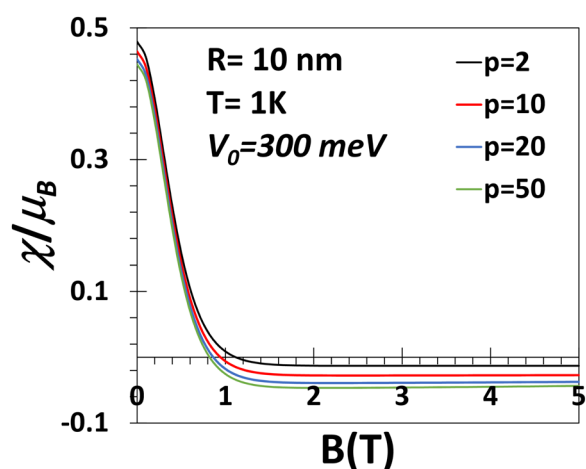


Figure 9. χ vs B for a GaAs QD with $V_0 = 300$ meV, $R = 10$ nm, $B = 1$ T and $T = 1$ K.

for a GaAs QD with $V_0 = 50$ meV has been plotted in Fig. 10. For low V_0 , χ is essentially independent of p below approximately $B = 1$ T. All these observations are consistent with Fig. 6.

The explicit p -dependence of the susceptibility is shown in Fig. 11 at $B = 1$ T for different values of $V_0 = 50$ meV. χ is found to increase with p at small p , attains a maximum and then starts decreasing. For low values of V_0 , χ is diamagnetic for all values of p . However, for $V_0 = 300$ meV, χ is negative for very small values of p and at a certain critical p , a transition occurs from the diamagnetic state to a paramagnetic state. Again χ attains a

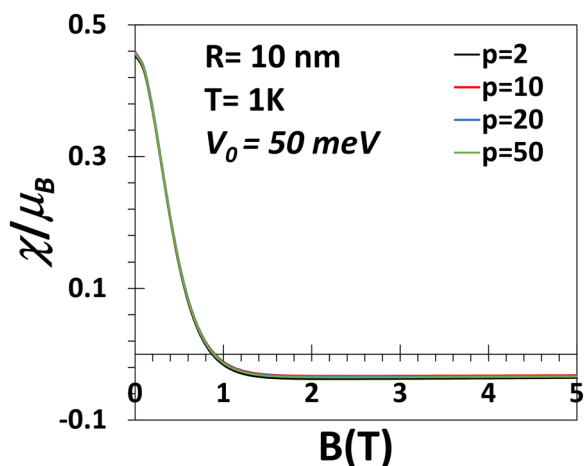


Figure 10. χ vs B for a GaAs QD with $V_0 = 50$ meV, $R = 10$ nm, $p = 2, 10, 20, 50$ at $T = 1$ K.

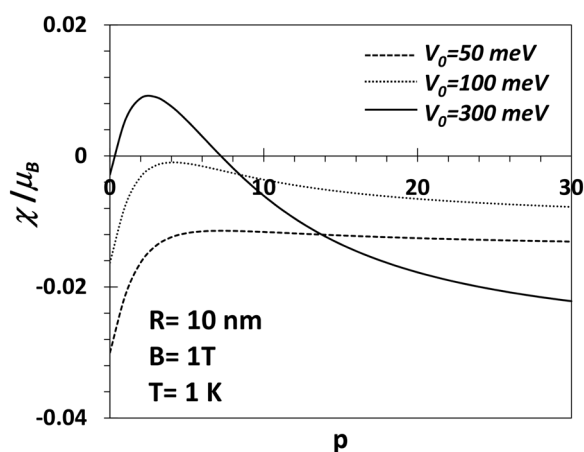


Figure 11. (χ/μ_B) vs p of a GaAs QD with $V_0 = 50, 100, 300$ meV, $R = 10$ nm, $B = 1$ T and $T = 1$ K.

maximum value at a certain value of p beyond which it decreases monotonically and becomes negative above a certain p . So if V_0 is made even larger, χ may be paramagnetic for a reasonable range of small values of p and then become diamagnetic at larger values of p . Thus we can have a re-entrant behaviour in the diamagnetic phase of a GaAs QD at low temperature and large V_0 .

Figure 12 shows the behavior of heat capacity (C/k_B) of a GaAs QD as a function of T for several values of V_0 and p at $T = 1$ K. Clearly, the heat capacity is independent of p and V_0 . Though at high magnetic field, the heat capacity is zero at low temperature, at low magnetic field ($B = 1$ T), C is zero up to a certain value of T beyond which it increases with T . This can be easily explained from fundamental physics. At $B = 1$ T, the system would require high energy to go to the excited states. At very low temperatures this energy is not available and therefore specific heat is expected to be zero. Nammas *et al.*⁴³ have calculated the specific heat of a few-electron interacting QD using static fluctuation approximation and our result qualitatively agrees with their result.

In Fig. 13, we plot the average persistent current (I) as a function of p for $B = 1$, $T = 1$ for a GaAs QD with $R = 10$ nm and $V_0 = 50, 100$ and 300 meV. We observe that at low temperature ($T = 1$ K), the persistent current is diamagnetic and its magnitude increases with decreasing V_0 . However the persistent current is independent of the shape of the confinement potential.

Conclusions

In conclusion, we have studied in this work the effect of the shape of the confinement potential on the electronic, thermodynamic, magnetic and transport properties of a GaAs QD at low temperature using a power-exponential model for quantum confinement. We first observe that the GS energy decreases with the increase in p which is an expected behaviour as the potential flattens with increasing p . The GS magnetization turns out to be diamagnetic which is also an expected behaviour for a binding potential in the GS. In keeping with the above results, the GS diamagnetic susceptibility also increases with the magnetic field.

Since our approximation is not so good for higher excited states, we have calculated the thermodynamic quantities only at very low temperature (at $T = 1$ K) because then, only the low-lying states will contribute. Our results show that even at low temperature the average energy decreases with increasing p at low p and saturates

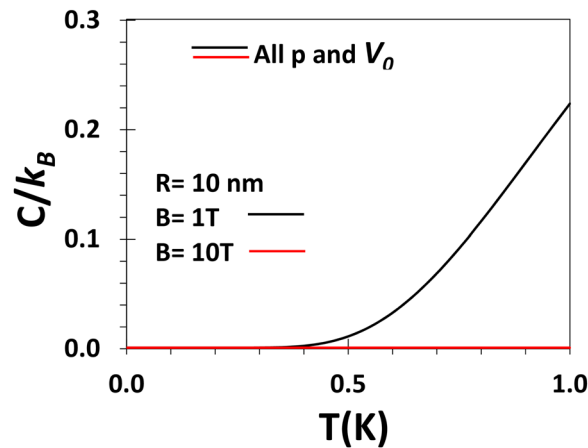


Figure 12. C/k_B vs T for $B = 1$ and 10 T for a GaAs QD with $R = 10$ nm, and different values of p and V_0 .

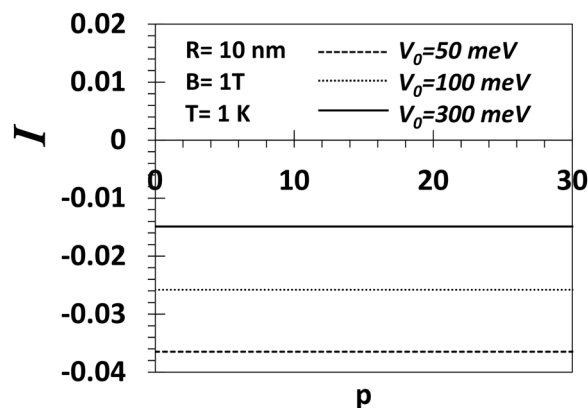


Figure 13. Persistent current (I) (in unit of $e\omega_n/e\hbar$) vs p for $B = 1$ T, $T = 1$ K for a GaAs QD with $V_0 = 50, 100$ and 300 meV.

to a constant value as p increases. The average energy, however, increases with the increase in the depth of the potential V_0 at small p , though at large p , the average energy becomes almost independent of V_0 . We have shown that at low temperature, the heat capacity of a GaAs QD is independent of the shape and depth of the confinement potential.

At $T = 1$ K, we have shown that χ is paramagnetic below a certain value of the magnetic field beyond which the system becomes diamagnetic. At small V_0 and small B (less than 1 T), χ is essentially independent of p . We have studied the variation of χ as a function of p explicitly at $T = 1$ K, $B = 1$ T and for three values of V_0 . In all cases, χ increases with p at small p , attains a maximum and then starts decreasing. For low values of V_0 ($50, 100$ meV), χ , however, remains always diamagnetic. For $V_0 = 300$ meV, χ is diamagnetic at small p , becomes paramagnetic as p exceeds a certain critical value and finally again becomes as p exceeds another critical value. So if V_0 is made still larger, χ may be paramagnetic even for small values of p and become diamagnetic at a larger value of p . Thus there exists a window of p values in which the re-entrant behaviour can show up. However, at very low temperature and large p , χ is never paramagnetic.

Finally we have shown that at low temperature, the persistent current in a GaAs QD is diamagnetic in nature and its magnitude increases with decreasing V_0 . It is however independent of p for the parameter values considered in this work.

Received: 14 November 2018; Accepted: 7 October 2019;

Published online: 01 November 2019

References

1. Kastner, M. A. The single-electron transistor. *Reviews of Modern Physics* **64**, 849–858 (1992).
2. Mukhopadhyay, S. & Chatterjee, A. Path-Integral Approach For Electron-Phonon Interaction Effects in Harmonic Quantum Dots. *Int J Mod Phys B* **10**, 2781–2796 (1996).
3. Mukhopadhyay, S. & Chatterjee, A. Polaronic enhancement in the ground-state energy of an electron bound to a Coulomb impurity in a parabolic quantum dot. *Phys Rev B* **55**, 9279 (1997).
4. Mukhopadhyay, S. & Chatterjee, A. Relaxed and effective-mass excited states of a quantum-dot polaron. *Phys Rev B* **58**, 2088 (1998).

5. Mukhopadhyay, S. & Chatterjee, A. Suppression of Zeeman splitting in a GaAs quantum dot. *Phys Rev B* **59**, R7833 (1999).
6. Mukhopadhyay, S. & Chatterjee, A. The ground and the first excited states of an electron in a multidimensional polar semiconductor quantum dot: an all-coupling variational approach. *Journal of Physics: Condensed Matter* **11**, 2071 (1999).
7. Krishna, R. P. M. & Chatterjee, A. Effect of electron–phonon interaction on the electronic properties of an axially symmetric polar semiconductor quantum wire with transverse parabolic confinement. *Physica B: Condensed Matter* **358**, 191–200 (2005).
8. Krishna, P. M. & Chatterjee, A. Polaronic effects in a polar semiconductor quantum strip with transverse parabolic confinement. *Physica E: Low-dimensional Systems and Nanostructures* **30**, 64–68 (2005).
9. Krishna, P. M., Mukhopadhyay, S. & Chatterjee, A. Polaronic effects in asymmetric quantum wire: An all-coupling variational approach. *Solid state communications* **138**, 285–289 (2006).
10. Krishna, P. M., Mukhopadhyay, S. & Chatterjee, A. Bipolaronic phase in polar semiconductor quantum dots: An all-coupling approach. *Physics Letters A* **360**, 655–658 (2007).
11. Mukhopadhyaya, S., Boyacioglu, B., Saglam, M. & Chatterjee, A. Quantum size effect on the phonon-induced Zeeman splitting in a GaAs quantum dot with Gaussian and parabolic confining potentials. *Physica E* **40**, 2776–2782 (2008).
12. Sanjeev Kumar, D., Mukhopadhyay, S. & Chatterjee, A. Effect of Rashba interaction and Coulomb correlation on the ground state energy of a GaAs quantum dot with parabolic confinement. *Physica E: Low-dimensional Systems and Nanostructures* **47**, 270–274 (2013).
13. Kumar, D. S., Mukhopadhyay, S. & Chatterjee, A. Magnetization and susceptibility of a parabolic InAs quantum dot with electron–electron and spin–orbit interactions in the presence of a magnetic field at finite temperature. *Journal of Magnetism and Magnetic Materials* **418**, 169–174 (2016).
14. Boda, A., Kumar, D. S., Sankar, I. & Chatterjee, A. Effect of electron–electron interaction on the magnetic moment and susceptibility of a parabolic GaAs quantum dot. *Journal of Magnetism and Magnetic Materials* **418**, 242–247 (2016).
15. Heitmann, D., Bollweg, K., Gudmundsson, V., Kurth, T. & Riege, S. Far-infrared spectroscopy of quantum wires and dots, breaking Kohn’s theorem. *Physica E: Low-dimensional Systems and Nanostructures* **1**, 204–210 (1997).
16. Miller, B. T. *et al.* Few-electron ground states of charge-tunable self-assembled quantum dots. *Phys Rev B* **56**, 6764 (1997).
17. Adamowski, J., Sobkowicz, M., Szafran, B. & Bednarek, S. Electron pair in a Gaussian confining potential. *Phys Rev B* **62**, 4234–4237 (2000).
18. Gu, J. & Liang, J. Q. Energy spectra of D– centres quantum dots in a Gaussian potential. *Physics Letters A* **335**, 451–456 (2005).
19. Boyacioglu, B., Saglam, M. & Chatterjee, A. Two-electron singlet states in semiconductor quantum dots with Gaussian confinement: a single-parameter variational calculation. *J Phys-Condens Mat* **19**, 456217 (2007).
20. Xie, W. F. Binding energy of an off-center hydrogenic donor in a spherical Gaussian quantum dot. *Physica B* **403**, 2828–2831 (2008).
21. Yuan-Peng, B. & Wen-Fang, X. Binding Energy of D– and D0 Centers Confined by Spherical Quantum Dots. *Communications in Theoretical Physics* **50**, 1449 (2008).
22. Gomez, S. S. & Romero, R. H. Binding energy of an off-center shallow donor D– in a spherical quantum dot. *Physica E: Low-dimensional Systems and Nanostructures* **42**, 1563–1566 (2010).
23. Gharaati, A. & Khordad, R. A new confinement potential in spherical quantum dots: modified Gaussian potential. *Superlattice Microst* **48**, 276–287 (2010).
24. Boyacioglu, B. & Chatterjee, A. Heat capacity and entropy of a GaAs quantum dot with Gaussian confinement. *Journal of Applied Physics* **112**, 083514 (2012).
25. Boyacioglu, B. & Chatterjee, A. Magnetic Properties of Semiconductor Quantum Dots with Gaussian Confinement. *Int J Mod Phys B* **26**, 1250018 (2012).
26. Boyacioglu, B. & Chatterjee, A. Persistent current through a semiconductor quantum dot with Gaussian confinement. *Physica B: Condensed Matter* (2012).
27. Boyacioglu, B. & Chatterjee, A. Dia- and paramagnetism and total susceptibility of GaAs quantum dots with Gaussian confinement. *Physica E* **44**, 1826–1831 (2012).
28. Boda, A. & Chatterjee, A. Ground state and binding energies of (D0), (D–) centres and resultant dipole moment of a (D–) centre in a GaAs quantum dot with Gaussian confinement. *Physica E: Low-dimensional Systems and Nanostructures* **45**, 36–40 (2012).
29. Boda, A., Boyacioglu, B. & Chatterjee, A. Ground state properties of a two-electron system in a three-dimensional GaAs quantum dot with Gaussian confinement in a magnetic field. *Journal of Applied Physics* **114**, 044311 (2013).
30. Boda, A. & Chatterjee, A. Effect of an external magnetic field on the binding energy, magnetic moment and susceptibility of an off-centre donor complex in a Gaussian quantum dot. *Physica B: Condensed Matter* **448**, 244–246 (2014).
31. Boda, A., Gorre, M. & Chatterjee, A. Effect of external magnetic field on the ground state properties of D– centres in a Gaussian quantum dot. *Superlattice Microst* **71**, 261–274 (2014).
32. Boda, A. & Chatterjee, A. The Binding Energy and Magnetic Susceptibility of an Off-Centre D0 Donor in the Presence of a Magnetic Field in a GaAs Quantum Dot with Gaussian Confinement: An Improved Treatment. *Journal of nanoscience and nanotechnology* **15**, 6472–6477 (2015).
33. Kumar, D. S., Boda, A., Mukhopadhyay, S. & Chatterjee, A. Effect of Rashba spin–orbit interaction on the ground state energy of a D0 centre in a GaAs quantum dot with Gaussian confinement. *Superlattice Microst* **88**, 174–179 (2015).
34. Boda, A., Boyacioglu, B., Erkaslan, U. & Chatterjee, A. Effect of Rashba spin–orbit coupling on the electronic, thermodynamic, magnetic and transport properties of GaAs, InAs and InSb quantum dots with Gaussian confinement. *Physica B: Condensed Matter* **498**, 43–48 (2016).
35. Boda, A. & Chatterjee, A. Transition energies and magnetic properties of a neutral donor complex in a Gaussian GaAs quantum dot. *Superlattice Microst* **97**, 268–276 (2016).
36. Jahan, K. L., Boda, A., Shankar, I., Raju, C. N. & Chatterjee, A. Magnetic field effect on the energy levels of an exciton in a GaAs quantum dot: Application for excitonic lasers. *Scientific reports* **8**, 5073 (2018).
37. Sharma, H. K., Boda, A., Boyacioglu, B. & Chatterjee, A. Electronic and magnetic properties of a two-electron Gaussian GaAs quantum dot with spin-Zeeman term: A study by numerical diagonalization. *Journal of Magnetism and Magnetic Materials* **469**, 171–177 (2019).
38. Ciurla, M., Adamowski, J., Szafran, B. & Bednarek, S. Modelling of confinement potentials in quantum dots. *Physica E: Low-dimensional Systems and Nanostructures* **15**, 261–268 (2002).
39. Kwaśniewski, A. & Adamowski, J. Effect of confinement potential shape on exchange interaction in coupled quantum dots. *Journal of Physics: Condensed Matter* **20**, 215208 (2008).
40. Xie, W. Potential-shape effect on photoionization cross section of a donor in quantum dots. *Superlattice Microst* **65**, 271–277 (2014).
41. Chakraborty, T. *Quantum Dots: A Survey of the Properties of Artificial Atoms*. (Elsevier Science, 1999).
42. Knoss, R. W. *Quantum Dots: Research, Technology and Applications*. (Nova Science Publishers, 2008).
43. Nammias, F., Sandouqa, A., Ghassib, H. & Al-Sugheir, M. Thermodynamic properties of two-dimensional few-electrons quantum dot using the static fluctuation approximation (SFA). *Physica B: Condensed Matter* **406**, 4671–4677 (2011).

Author contributions

K.L.J. and B.B. performed the analytical and numerical calculations. K.L.J. wrote the draft version of the manuscript. B.B. wrote the final manuscript. A.C. supervised the work.

Competing interests

The authors declare no competing interests.

Additional information

Correspondence and requests for materials should be addressed to B.B.

Reprints and permissions information is available at www.nature.com/reprints.

Publisher's note Springer Nature remains neutral with regard to jurisdictional claims in published maps and institutional affiliations.



Open Access This article is licensed under a Creative Commons Attribution 4.0 International License, which permits use, sharing, adaptation, distribution and reproduction in any medium or format, as long as you give appropriate credit to the original author(s) and the source, provide a link to the Creative Commons license, and indicate if changes were made. The images or other third party material in this article are included in the article's Creative Commons license, unless indicated otherwise in a credit line to the material. If material is not included in the article's Creative Commons license and your intended use is not permitted by statutory regulation or exceeds the permitted use, you will need to obtain permission directly from the copyright holder. To view a copy of this license, visit <http://creativecommons.org/licenses/by/4.0/>.

© The Author(s) 2019